DOI:
10.1016/j.ejpn.2018.03.003

Document Version
Peer reviewed version

Accepted Manuscript

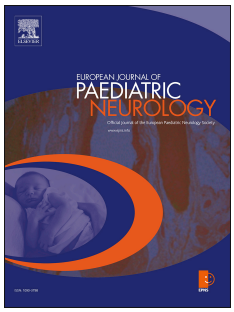

Resting State Cerebral Blood Flow with Arterial Spin Labeling MRI in Developing Human Brains

Feng Liu, Yunsuo Duan, Bradley S. Peterson, Iris Asllani, Fernando Zelaya, David Lythgoe, Alayar Kangarlu

PII: S1090-3798(17)31732-4

DOI: 10.1016/j.ejpn.2018.03.003

Reference: YEJPN 2398

To appear in: *European Journal of Paediatric Neurology*

Received Date: 15 August 2017

Revised Date: 25 January 2018

Accepted Date: 18 March 2018

Please cite this article as: Liu F, Duan Y, Peterson BS, Asllani I, Zelaya F, Lythgoe D, Kangarlu A, Resting State Cerebral Blood Flow with Arterial Spin Labeling MRI in Developing Human Brains, *European Journal of Paediatric Neurology* (2018), doi: 10.1016/j.ejpn.2018.03.003.

Resting State Cerebral Blood Flow with Arterial Spin Labeling MRI in Developing Human Brains

Authors
Feng Liu [1,2], Yunsuo Duan [1,2], Bradley S. Peterson [3,4] Iris Asllani [5], Fernando Zelaya [6], David Lythgoe [6], Alayar Kangarlu [1,2 *]

1. Department of Psychiatry, Columbia University, New York, NY
2. New York State Psychiatric Institute, New York, NY
3. Institute for the Developing Mind, Children's Hospital Los Angeles, Los Angeles, CA
4. The Keck School of Medicine, the University of Southern California, Los Angeles, CA
5. The Kate Gleason College of Engineering, Rochester Institute of Technology, Rochester, NY
6. Institute of Psychiatry, Psychology and Neuroscience, King's College, London, U.K.

*Correspondence to:
Alayar Kangarlu
MRI Unit, New York State Psychiatric Institute and Columbia University, 1051 Riverside Drive, New York, NY 10032, USA
(Tel) 646-774-7258
(Email) alayar.kangarl@nyspi.columbia.edu

Abstract

The development of brain circuits is coupled with changes in neurovascular coupling, which refers to the close relationship between neural activity and cerebral blood flow (CBF). Studying the characteristics of CBF during resting state in developing brain can be a complementary way to understand the functional connectivity of the developing brain. Arterial spin labeling (ASL), as a noninvasive MR technique, is particularly attractive for studying cerebral perfusion in children and even newborns. We have collected pulsed ASL data in resting state for 47 healthy subjects from young children to adolescence (aged from 6 to 20 years old). In addition to studying the developmental change of static CBF maps during resting state, we also analyzed the CBF time series to reveal the dynamic characteristics of CBF in differing age groups. We used the seed-based correlation analysis to examine the temporal relationship of CBF time series between the selected ROIs and other brain regions. We have shown the developmental patterns in both static CBF maps and dynamic characteristics of CBF. While higher CBF of default mode network (DMN) in all age groups supports that DMN is the prominent active network during the resting state, the CBF connectivity patterns of some typical resting state networks show distinct patterns of metabolic activity during the resting state in the developing brains.

Keywords
ASL, CBF, Resting State, cerebral perfusion, brain development

Introduction

Brain maturation (both structural and functional) continues through childhood and adolescence into early adulthood. The development of brain circuits is coupled with changes in neurovascular coupling [1], which refers to the close relationship between neural activity and cerebral blood flow (CBF) [2]. Regional neural activity produces an increase of regional blood flow to meet its energy needs. Thus cerebral metabolism and the regional functional activity are highly correlated to CBF, i.e., cerebral perfusion. Therefore, cerebral perfusion can be used as an indirect measure of the energy demand in the brain [3]. Characterization of the regional change in cerebral metabolism during brain development is very important because it enhances our understanding of structure-function relationships in normal and diseased brains. Since cerebral perfusion reflects cerebral metabolic demand, it is important to study the trajectory of cerebral perfusion in the developing brain.

Studies have shown that regional CBF (rCBF) is closely coupled with glucose utilization, oxygen consumption, and aerobic glycolysis in resting brains [4,5]. Using positron-emission tomography (PET) imaging, changes in rCBF have been shown to be proportional to changes in regional glucose metabolism due to task activation [6]. Furthermore, the changes of regional metabolism and regional CBF throughout childhood have been measured with PET, single-photon emission computed tomography (SPECT), or perfusion computed tomography (CT) [7-9]. However, CT and nuclear medicine techniques are expensive and require injection of radioactive tracers or contrast agents, which are costly, uncomfortable, and potentially harmful. As a result, these methods are not ideal for studying brain perfusion in healthy children. Though the period from birth to adolescence is the most important in brain development, pediatric CBF data are still sparse due to a lack of consensus on the technique of choice for measuring CBF and limited availability of CBF techniques.

Arterial spin labeling (ASL) is a noninvasive MR technique that has been developed to evaluate cerebral perfusion [10]. ASL has been extensively validated against the nuclear medicine methods (PET and SPECT) and other MRI perfusion technique, namely dynamic susceptibility contrast MRI (DSC-MRI) [11,12]. In ASL, arterial water is used as an endogenous tracer. To distinguish static tissue water in the brain from the flowing arterial water, the water spins in the blood are inverted prior to arrival in an area proximal to the region of interest. Because ASL does not require intravenous injection of radioactive tracers or contrast agents, it can be repeated safely over time. Therefore, ASL is particularly attractive for studying cerebral perfusion in children, even newborns and infants. Since CBF maps at different ages can be used to evaluate the trajectory of brain perfusion in the developing brain, ASL MRI has been used as a biomarker for functional brain development. Several studies have investigated developmental changes of brain perfusion using ASL at 1.5 T and 3 T [13-16]. Nevertheless, these studies only focused on the developmental changes of static CBF, not the dynamic characteristics of CBF.

Historically, based on how the labeling is done, ASL techniques have been classified as continuous ASL (CASL) and pulsed ASL (PASL) before the recent developments of pseudo-continuous ASL (pCASL) and velocity selective ASL (VSASL). Until recently, PASL has been more widely used than CASL because of its easier implementation. Though CASL has higher signal-to-noise ratio (SNR) than PASL, CASL requires a long radio frequency (RF) labeling pulse (typically ~2s), which is taxing on the hardware. Therefore, CASL is not widely implemented on many commercial MR scanners. On the contrary, PASL uses short RF labeling pulse (usually 10-15 ms) and can be implemented easily on commercial MR scanners [17]. Nevertheless, a notable advantage of PASL methods in investigations of brain perfusion in infants and young kids is the reduced risk of excessive RF power deposition from the labelling

pulse, since the duty cycle of this pulse over repetition time (TR) is very low [16]. In our study, we chose a multi-slice PASL method to collect CBF time courses in resting state from healthy subjects at differing ages.

The advantage of collecting baseline CBF images is that the time-series can be used to investigate the functional connectivity of brain perfusion. Resting state fMRI is becoming more popular in studying the development of functional brain connectivity. Resting state fMRI provides a method without the use of external tasks, which is more convenient than performing task activation fMRI in infants and younger children. Resting state ASL is both complementary and advantageous to blood-oxygen-level dependent (BOLD) fMRI resting state alone. Compared to the complexity of the BOLD signal, the ASL signal follows the time course of a single physiological parameter (CBF). Most relevantly, ASL is not dependent on baseline changes, and therefore is less affected by scanner drifts [18]. Consequently, ASL can detect changes in the very low frequency range, which is not achievable with BOLD fMRI. Regional CBF can be used as a reasonable surrogate of metabolism in resting states. BOLD fMRI data and ASL perfusion contrasts have been used to investigate the relationship between functional connectivity strength (FCS) and rCBF during resting and task states in adult brains [19,20]. These studies have evaluated the correlations between resting BOLD fMRI and CBF. They have suggested that resting BOLD fMRI measures are coupled with regional CBF, which reflects the underlying spontaneous brain activity.

Since analysis of CBF time series can reveal the characteristics of the development of functional connectivity, we used the seed-based correlation analysis to examine the temporal relationship of CBF between the selected ROIs and other brain regions in the subjects aged from 6 years old to 20 years old. In this study, we explore the feasibility that with the use of noninvasive ASL

technique, the dynamic characteristics of CBF in developing brain can be used as a complementary way to understand the functional connectivity of the developing brain, in addition to the developmental changes of static rCBF.

Materials and Methods

MRI Acquisition

MRI data used in this study were extracted from MRI data pool of healthy controls from several studies done on the same scanner. All MRI scans were approved by the local IRB, and informed consent was obtained from parents for subjects under the age of 18 and from subjects older than 18. During the resting state ASL scans, all subjects were instructed to stay awake and keep eyes close. We have collected ASL data for 47 healthy subjects: 6-8 year-old (N=8, 3 males, 7.6±0.6 years), 9-11 year-old (N=9, 4 males, 10.7±0.9 years), 12-14 year-old (N=10, 4 males, 12.8±0.8 years), 15-17 year-old (N=10, 5 males, 16.1±0.8 years), and 18-20 year-old (N=10, 5 males, 19.0±0.5 years). All scans were performed on a GE Signa 3T HDx scanner (GE Healthcare, Chicago, USA) with an 8-channel receive-only head coil (Invivo Corporation, Gainesville, USA). A Pulsed ASL (PASL) perfusion sequence was implemented using a proximal inversion with control for off-resonance effects (PICORE) quantitative imaging of perfusion using a single subtraction (QUIPSS II) sequence [21]. Inversion of arterial spins was achieved using a 15ms hyperbolic secant RF pulse over a slab of 9cm thickness, located 2cm below the image volume. The same PASL sequence has been used in a previous study with newborns on the same scanner [22]. A 2-D single-shot gradient-echo echo-planar imaging (EPI) sequence was used for image acquisition in axial-oblique orientation. The time to QUIPSS saturation pulse is TI1 = 600 ms and inversion time of the first slice is TI2 = 1300ms. Other acquisition parameters included: 3.75 x 3.75 mm^2 in-plane resolution, TE (echo time) = 26 ms, TR = 2300 ms, flip angle 90°, slice

thickness 6 mm, inter-slice spacing 0.5 mm. Eighteen slices were acquired sequentially from inferior to superior in the brain. Each ASL scan with 151 brain images (including 76 control images and 75 label images) and 5 dummies required 5 min 59 sec totally. A separate M0 scan using gradient-echo EPI with TR of 15s was acquired and used as a control image for quantification of CBF [21]. In addition to the ASL-related sequences, we acquired a 3-D T1-weighted structural image using inversion recovery prepared fast SPGR (IR-FSPGR) with spatial resolution of $(1mm)^3$. We also acquired a 2-D T1-weighted-fluid-attenuated inversion recovery (T1-FLAIR) images with the same slice placement as the ASL sequence had, but with higher in-plane resolution ($0.94 \times 0.94\ mm^2$).

Data Processing

The PASL data were preprocessed for head motion correction and spatial smoothing with an 8-mm Gaussian kernel via Statistical Parametric Mapping (SPM) software [23]. Any volumes with large motion (translation larger than 2mm and/or rotation larger than 1.5° between consecutive volumes) were removed. Data with large motion in more than 10% of volumes were excluded. After perfusion-weighted images were calculated by surround subtraction in which each label image is subtracted from the average of its two nearest control images, CBF maps were then calculated as described in [21,24,25]. For each participant, an average CBF map was obtained by averaging across the CBF time series. First we calculated the global CBF value for each participant. Some variability in the observed CBF values of differing subjects was likely because of the variability in labeling efficiency. Then to reduce such variability in CBF for the group analysis, the static CBF map of each subject was divided by the global CBF of that subject, so that the CBF map was converted to a relative CBF map [26].

The dynamic characteristics of CBF were examined by analyzing the time course of the PASL data. We used seed-based correlation analysis to examine the temporal relationship between the selected regions of interest (ROIs) and other brain regions. For seed ROIs, a small cluster of voxels were drawn in insula, posterior cingulate cortex (PCC)/precuneus, medial prefrontal cortex (MPFC)/anterior cingulate cortex (ACC), and thalamus, respectively, on the individual CBF map. All these regions have higher static CBF than the whole brain mean CBF, and are parts of resting state networks [4,27,28]. A neuroscientist with more than 10 years of experience checked the position of each seed ROI on the corresponding T1-FLAIR overlay image to make sure that it is in the correct position. The seed size for each ROI (3 voxels in the anterior region of right insula, 4 voxels in PCC/precuneus, 4 voxels in MPFC/ACC, and 4 voxels in right thalamus) was kept the same for all subjects. We extracted the CBF time series from the original PASL signals with reduced contamination from BOLD fluctuations [29,30]. The PASL data set was first high-pass filtered with a cutoff frequency of 1/4TR (0.1087Hz). Then the filtered time course was demodulated to low frequency by multiplying $cos(\pi n)$ (n is the scan index). This way we reduced the potential contamination from BOLD in analyzing CBF fluctuation brains during the resting state [29,30,22]. After extraction with reduced BOLD contamination, the time course of each voxel in the brain was correlated with the average time course of the seed ROI. Thus the correlation coefficient (CC) map is obtained for each subject. The correlation coefficient measures the strength of the linear relationship between the signal intensity in each voxel and that in selected seed ROI.

Data Analysis

We plotted the mean global CBF and the average static CBF maps for all the age groups. As a comparison, we also included the CBF results from a group of newborns (N=10, 0.5±0.1 months) obtained using the same method in a previous study [22].

For each age group, we used DARTEL toolbox in SPM [31] to create a group template using the T1-weighted structural images of all subjects in that group. Therefore we had age-specific templates, which were preferred for pediatric cohorts [32]. Then all static CBF maps in the same age group were normalized to the group template via SPM [33]. A voxel-wise one-sided one-sample t-test against 1 (=1 vs >1) was performed on the relative CBF maps for each age group. The regions with static CBF significantly higher than the global average can be identified. On the normalized CBF maps, we drew the ROIs in the regions which showed higher CBF than the whole-brain mean CBF in previous studies [4,30], such as MPFC/ACC, PCC/precuneus, thalamus, and insula. To study the dynamic characteristics of CBF, the correlation coefficient maps were also normalized to the corresponding group template. In each age group, a voxel-wise one-sided one-sample t-test was performed on the normalized individual CC maps to find out the regions highly correlated to the seed ROI.

Results

The average global CBF values across the age groups are shown in Fig. 1. The global CBF rises in the early childhood, and then falls in the late childhood.

The average relative CBF (relCBF) maps for different age groups are shown in Fig. 2. Here too, for comparison, we calculated the relative CBF maps acquired using similar method in newborns (N=10, 0.5±0.1 months) from a previous study [22]. For newborns, CBF is higher near the basal ganglia, temporal lobe, and PCC. For the other age groups (from 6 to 20 y.o.), the CBF

in PCC/precuneus, MPFC/ACC, thalamus, and insula, are higher than the global CBF of the whole brain. Fig. 3 shows the mean values of relative CBF in the ROIs within PCC/precuneus, MPFC/ACC, thalamus on both sides, and insula on both sides, all of which were chosen on the average relCBF maps in each age group. In groups 6-8 y.o., relCBF values in the posterior regions with relCBF >1 are greater than those in the anterior regions. In groups 9-11 y.o. and 12-14 y.o., relCBF around insula and MPFC/ACC become higher gradually. Then the pattern of relCBF remains similar for groups 15-17 y.o. and 18-20 y.o..

A voxel-wise one-sided one-sample t-test against 1 was performed on the relative CBF maps for each age group. Fig. 4 shows the regions with CBF significantly higher than global CBF ($P = 0.001$). We counted the number of voxels with relCBF>1 ($P = 0.001$) within the brain section defined by the top and bottom slices in Fig. 4, and calculated its percentage in total voxel number in this brain section (Fig. 5). Group 12-14 y.o. has the most extended region with relCBF>1 ($P = 0.001$) among all groups.

As described in Materials and Methods, the seed ROIs were selected in right insula, PCC/precuneus, MPFC/ACC, and right thalamus, respectively, on the individual CBF maps. For each seed ROI, the correlation coefficient (CC) was computed on a voxel-wise base for each participant. In each age group, a voxel-wise one-sided one-sample t-test CC>0.4 against CC=0.4 was performed on the individual CC maps normalized to the group template. Figs 6-9 shows the regions with CC>0.4 significantly (P=0.05). We also counted the percentage of voxels with CC>0.4 (P=0.05) in these CC maps (Figs. 6-9) within the same brain sections (between Slices #25 and #56) for differing age groups (Fig. 10). Figs. 6 and 10 show that the groups 12-14 y.o. and 15-17 y.o. have more extended regions correlated to the ROI seed in the insula. Figs. 7 and 10 show that as age increases, the region correlated to the seed ROI in PCC/precuneus becomes

more extended and peaks in adolescent group (15-17 y.o.). Fig. 8 shows that the region correlated to the seed ROI in MPFC/ACC is a large cluster in group 6-8 y.o.. As age increases (in group 18-20 y.o.), there are more regions showing correlation to the seed ROI, though each region is more refined. Fig. 9 shows that the region correlated to the seed ROI in thalamus does not change as dramatically as those regions correlated to the other seed ROIs.

Discussion

In this study, we used a PASL sequence and perfusion model based on parameters derived from healthy adults. As explained in [16], though optimizing the perfusion model for pediatric population is of importance due to large variability in pediatric age groups, it is still reasonable to do pediatric CBF quantification using adult model since the effects of changing values of some parameters such as blood T1 and blood-brain partition coefficient of water can be balanced by each other. Another factor may affect CBF quantification is the growth of neck during childhood. The growth of neck could affect the optimal position of tagging plane for best tagging efficiency in CASL or pCASL and therefore the position of tagging plane may need adjustment on an individual basis [34]. However, in the PASL sequence we used, a wide tagging slab (9 cm thick) was placed 2 cm below the imaging slab, which should be less sensitive to the effect of growth of neck.

ASL perfusion fMRI is an ideal method for developing biomarkers of functional brain development. Compared to PET and SPECT, a big advantage of ASL is its safety features. Most of PET and SPECT studies on children are in pseudo-clinical samples. Our samples are much more representative of healthy children. Although the PET studies and ours were cross-sectional,

ASL will be more amenable to longitudinal designs to identify true developmental trajectories in health and illness.

With the results from PASL, the trend of global CBF with age (Fig. 1) shows that CBF increases dramatically from birth to young childhood, and then gradually declines throughout adolescence. Our data on changes of regional CBF in resting state throughout the brain development is consistent with those results obtained in other studies [7,9,14,15]. Using PET, Chugani et al. (1987) showed that regional cerebral glucose metabolism increased from birth, peaking at ~9 years, followed by a decline to adult levels throughout the teenage years [8]. With SPECT, Chiron et al. (1992) showed that regional CBF increased from birth until 5 or 6 years old, and then decreased to adult levels between 15 and 19 years. Some recent studies using ASL MRI also shows similar trends [14,15]. The time needed to reach adult values differed for differing cortical regions. From developmental trajectories of regional CBF (Figs 2, 3, and 4), regional CBF increases with age in the frontal cortex and anterior cingulate cortex, which may reflect the later maturation of cortical regions associated with executive function and cognitive control [35]. Differences between older and younger individuals in CBF of MPFC and ACC could be interpreted as the need for recruiting the anterior insula in the developed brain that is absent in adolescents. Studies have shown lack of activation in anterior insula in adolescents [36]. The findings of higher CBF in insula and MPFC/ACC in adults is consistent with others' findings showing the anterior insula's involvement in regulatory behavior [37], which indicates greater functional connectivity in the prefrontal regions to the anterior insula in adults compared to adolescents. Absence of such association for young children and adolescents could be due to the lower connectivity of insula with dorsolateral prefrontal cortex (DLPFC) and dorsal anterior cingulate cortex (dACC) in early life than in adults. The differences in CBF is consistent with

prefrontal activation and connectivity that also supports the dysregulated behavior usually exhibited in children and adolescents.

In addition to the developmental changes of static rCBF, there are developmental patterns in the CC maps of the dynamic CBF changes between the selected seed ROIs and other brain regions (Figs. 6-9). These selected seed ROIs (in PCC/precuneus, MPFC/ACC, insula, and thalamus) are parts of resting state networks (RSN) [4,27,28]. There are already studies combining the BOLD fMRI data and ASL data to investigate the relationship between the functional connectivity and the rCBF during the resting state in adult brains [19,20]. In this paper, we demonstrate distinct CBF-based developmental patterns in pediatric age groups. PCC/precuneus seed-based network is a major part of default mode network (DMN) (Fig. 7), which has higher CBF than other RSNs in all age groups from 6-20 y.o. (Fig. 4) and show more extended regions in 15-17 y.o and 18-20 y.o. than in younger age groups (Figs. 7 and 10). Higher CBF in DMN supports that DMN is the most prominent active network during the resting state [19]. MPFC/ACC seed-based network in 18-20 y.o. group also shows pattern of auditory network (Fig. 8) [38] while those in younger age groups show less of it (Fig. 8). Our results show distinct connectivity patterns of metabolic activity in regions correlated to PCC/precuneus, MPFC/ACC, insula, and thalamus in the developing brains and could benefit from the results of the studies evaluating the correlations between resting BOLD fMRI and CBF [19,38,39]. Assuming that studies demonstrating that resting BOLD fMRI measures are coupled with regional CBF, our results suggests that the underlying metabolism of the spontaneous brain activity is different in young children (up to age 6) compared to adolescents and adults. While studies have shown correlation between BOLD and CBF in adults establishing the mechanism of neurovascular coupling in the adult brain but, to the best of our knowledge, such studies have not been carried out in children. As such, in the

light of our findings, studies comparing BOLD and CBF in the population of younger age and adolescence could shed light on the evolution of the mechanism of neurovascular coupling in the brain and provide more on the physiological basis of the development of human brain connectivity in general.

Conclusion

The resting-state CBF data is complementary to the resting-state BOLD fMRI data in studying the functional connectivity of the developing brain. We have demonstrated that by studying the changes in the characteristic of CBF obtained with ASL MRI, we can better understand the development of functional brain connectivity. With ASL becoming a standard sequence on commercial MRI scanners, more CBF data will be acquired using ASL MRI in clinical and research applications. Using methodology described here, we can establish the developmental patterns of cerebral perfusion, therefore the cerebral metabolism and functional brain connectivity, in both normal and disease brains.

Conflict of interest None.

References

1. Harris JJ, Reynell C, Attwell D (2011) The physiology of developmental changes in BOLD functional imaging signals. Dev Cogn Neuros-Neth 1 (3):199-216
2. Attwell D, Buchan AM, Charpak S, Lauritzen M, Macvicar BA, Newman EA (2010) Glial and neuronal control of brain blood flow. Nature 468 (7321):232-243
3. Raichle ME (1998) Behind the scenes of functional brain imaging: A historical and physiological perspective. P Natl Acad Sci USA 95 (3):765-772
4. Raichle ME, MacLeod AM, Snyder AZ, Powers WJ, Gusnard DA, Shulman GL (2001) A default mode of brain function. P Natl Acad Sci USA 98 (2):676-682
5. Vaishnavi SN, Vlassenko AG, Rundle MM, Snyder AZ, Mintun MA, Raichle ME (2010) Regional aerobic glycolysis in the human brain. P Natl Acad Sci USA 107 (41):17757-17762

6. Fox PT, Raichle ME, Mintun MA, Dence C (1988) Nonoxidative glucose consumption during focal physiologic neural activity. Science 241 (4864):462-464
7. Chiron C, Raynaud C, Maziere B, Zilbovicius M, Laflamme L, Masure MC, Dulac O, Bourguignon M, Syrota A (1992) Changes in regional cerebral blood flow during brain maturation in children and adolescents. J Nucl Med 33 (5):696-703
8. Chugani HT, Phelps ME, Mazziotta JC (1987) Positron emission tomography study of human brain functional development. Ann Neurol 22 (4):487-497
9. Wintermark M, Lepori D, Cotting J, Roulet E, van Melle G, Meuli R, Maeder P, Regli L, Verdun FR, Deonna T, Schnyder P, Gudinchet F (2004) Brain perfusion in children: Evolution with age assessed by quantitative perfusion computed tomography. Pediatrics 113 (6):1642-1652
10. Williams DS, Detre JA, Leigh JS, Koretsky AP (1992) Magnetic-Resonance-Imaging of Perfusion Using Spin Inversion of Arterial Water. P Natl Acad Sci USA 89 (1):212-216
11. Vonken E-jPA, Beekman FJ, Bakker CJG, Viergever MA (1999) Maximum likelihood estimation of cerebral blood flow in dynamic susceptibility contrast MRI. Magnet Reson Med 41 (2):343-350
12. Wirestam R, Andersson L, Ostergaard L, Bolling M, Aunola J-P, Lindgren A, Geijer B, Holtås S, Ståhlberg F (2000) Assessment of regional cerebral blood flow by dynamic susceptibility contrast MRI using different deconvolution techniques. Magnet Reson Med 43 (5):691-700
13. Miranda MJ, Olofsson K, Sidaros K (2006) Noninvasive measurements of regional cerebral perfusion in preterm and term neonates by magnetic resonance arterial spin labeling. Pediatr Res 60 (3):359-363
14. Biagi L, Abbruzzese A, Bianchi MC, Alsop DC, Del Guerra A, Tosetti M (2007) Age dependence of cerebral perfusion assessed by magnetic resonance continuous arterial spin labeling. J Magn Reson Imaging 25 (4):696-702
15. Taki Y, Hashizume H, Sassa Y, Takeuchi H, Wu K, Asano M, Asano K, Fukuda H, Kawashima R (2011) Correlation Between Gray Matter Density-Adjusted Brain Perfusion and Age Using Brain MR Images of 202 Healthy Children. Hum Brain Mapp 32 (11):1973-1985
16. Wang JJ, Licht DJ, Jahng GH, Liu CS, Rubin JT, Haselgrove J, Zimmerman RA, Detre JA (2003) Pediatric perfusion imaging using pulsed arterial spin labeling. J Magn Reson Imaging 18 (4):404-413
17. Borogovac A, Asllani I (2012) Arterial Spin Labeling (ASL) fMRI: Advantages, Theoretical Constrains and Experimental Challenges in Neurosciences. International Journal of Biomedical Imaging 2012
18. Borogovac A, Habeck C, Small SA, Asllani I (2010) Mapping brain function using a 30-day interval between baseline and activation: a novel arterial spin labeling fMRI approach. J Cerebr Blood F Met 30 (10):1721-1733
19. Li ZJ, Zhu YS, Childress AR, Detre JA, Wang Z (2012) Relations between BOLD fMRI-Derived Resting Brain Activity and Cerebral Blood Flow. Plos One 7 (9)
20. Liang X, Zou QH, He Y, Yang YH (2013) Coupling of functional connectivity and regional cerebral blood flow reveals a physiological basis for network hubs of the human brain. P Natl Acad Sci USA 110 (5):1929-1934
21. Wong EC, Buxton RB, Frank LR (1998) Quantitative imaging of perfusion using a single subtraction (QUIPSS and QUIPSS II). Magnet Reson Med 39 (5):702-708

22. Liu F, Wang Z, Duan Y, Zelaya F, Lythgoe DJ, Kangarlu A, Peterson BS Static and dynamic characteristics of resting state CBF in newborn infants. In: Joint Annual Meeting ISMRM - ESMRMB, Stockholm, 2010.
23. Friston KJ (2007) Statistical parametric mapping : the analysis of funtional brain images. 1st edn. Elsevier/Academic Press, Amsterdam ; Boston
24. Wong EC, Buxton RB, Frank LR (1997) Implementation of quantitative perfusion imaging techniques for functional brain mapping using pulsed arterial spin labeling. Nmr Biomed 10 (4-5):237-249
25. Lu HZ, Donahue MJ, van Zijl PCM (2006) Detrimental effects of BOLD signal in arterial spin Labeling fMRI at high field strength. Magnet Reson Med 56 (3):546-552
26. Wang Z, Fernandez-Seara M, Alsop DC, Liu WC, Flax JF, Benasich AA, Detre JA (2008) Assessment of functional development in normal infant brain using arterial spin labeled perfusion MRI. Neuroimage 39 (3):973-978
27. Damoiseaux JS, Rombouts SARB, Barkhof F, Scheltens P, Stam CJ, Smith SM, Beckmann CF (2006) Consistent resting-state networks across healthy subjects. P Natl Acad Sci USA 103 (37):13848-13853
28. Tang L, Ge Y, Sodickson DK, Miles L, Zhou Y, Reaume J, Grossman RI (2011) Thalamic resting-state functional networks: disruption in patients with mild traumatic brain injury. Radiology 260 (3):831-840
29. Chuang KH, Van Gelderen P, Merkle H, Bodurka J, Ikonomidou VN, Koretsky AP, Duyn JH, Talagala SL (2008) Mapping resting-state functional connectivity using perfusion MRI. Neuroimage 40 (4):1595-1605
30. Zou QH, Wu CW, Stein EA, Zang YF, Yang YH (2009) Static and dynamic characteristics of cerebral blood flow during the resting state. Neuroimage 48 (3):515-524
31. Ashburner J (2007) A fast diffeomorphic image registration algorithm. Neuroimage 38 (1):95-113
32. Sanchez CE, Richards JE, Almli CR (2012) Age-Specific MRI Templates for Pediatric Neuroimaging. Dev Neuropsychol 37 (5):379-399
33. Friston KJ, Holmes AP, Worsley KJ, Poline JP, Frith CD, Frackowiak RSJ (1994) Statistical parametric maps in functional imaging: A general linear approach. Hum Brain Mapp 2 (4):189-210
34. Shin DD, Liu TT, Wong EC, Shankaranarayanan A, Jung Y (2012) Pseudocontinuous arterial spin labeling with optimized tagging efficiency. Magn Reson Med 68 (4):1135-1144
35. Ardila A (2008) On the evolutionary origins of executive functions. Brain Cogn 68 (1):92-99
36. Strang NM, Pruessner J, Pollak SD (2011) Developmental changes in adolescents' neural response to challenge. Dev Cogn Neuros-Neth 1 (4):560-569
37. Medford N, Critchley HD (2010) Conjoint activity of anterior insular and anterior cingulate cortex: awareness and response. Brain Struct Funct 214 (5-6):535-549
38. Zhu SH, Fang Z, Hu SY, Wang Z, Rao HY (2013) Resting State Brain Function Analysis Using Concurrent BOLD in ASL Perfusion fMRI. Plos One 8 (6)
39. Jann K, Gee DG, Kilroy E, Schwab S, Smith RX, Cannon TD, Wang DJJ (2015) Functional connectivity in BOLD and CBF data: Similarity and reliability of resting brain networks. Neuroimage 106:111-122

Figure Captions

Fig. 1 The mean values and standard deviations of global CBF in differing age groups: 6-8 year-old (N=8, 7.6±0.6 years), 9-11 year-old (N=9, 10.7±0.9 years), 12-14 year-old (N=10, 12.8±0.8 years), 15-17 year-old (N=10, 16.1±0.8 years), and 18-20 year-old (N=10, 19.0±0.5 years). As a comparison, the mean global CBF from a group of newborns (N=10, 0.5±0.1 months) is also included [22].

Fig. 2 The average relative CBF maps of three different slices from inferior to superior (top row to bottom row) in different age groups. As a comparison, the average relative CBF maps for a group of ten newborns (N=10, 0.5±0.1 months) is shown on the 1st column.

Fig. 3 The mean relCBF values in the ROIs selected within different brain regions (PCC/precuneus, MPFC/ACC, thalamus on both sides, and insula on both sides) for each age group.

Fig. 4 The regions with relCBF>1 (P=0.001) overlaid on average relCBF maps for each age group. It shows the regions with CBF significantly higher than global CBF.

Fig. 5 Percentage of voxels with relCBF>1 (P=0.001) within the brain section defined by the top and bottom slices in Fig. 4 for each age group.

Fig. 6 For CC maps obtained with ROI seed-based analysis (seed ROI selected in right insula), the regions with CC>0.4 (P=0.05) for differing age groups.

Fig. 7 For CC maps obtained with ROI seed-based analysis (seed ROI selected in PCC/precuneus), the regions with CC>0.4 (P=0.05) for differing age groups.

Fig. 8 For CC maps obtained with ROI seed-based analysis (seed ROI selected in MPFC/ACC), the regions with CC>0.4 (P=0.05) for differing age groups.

Fig. 9 For CC maps obtained with ROI seed-based analysis (seed ROI selected in right thalamus), the regions with CC>0.4 (P=0.05) for differing age groups.

Fig. 10 Percentage of voxels with CC>0.4 (P=0.05) in CC maps with differing seed ROIs (in right insula, PCC/precuneus, MPFC/ACC, and right thalamus, respectively) (Figs. 6-9) within the same brain sections for differing age groups.

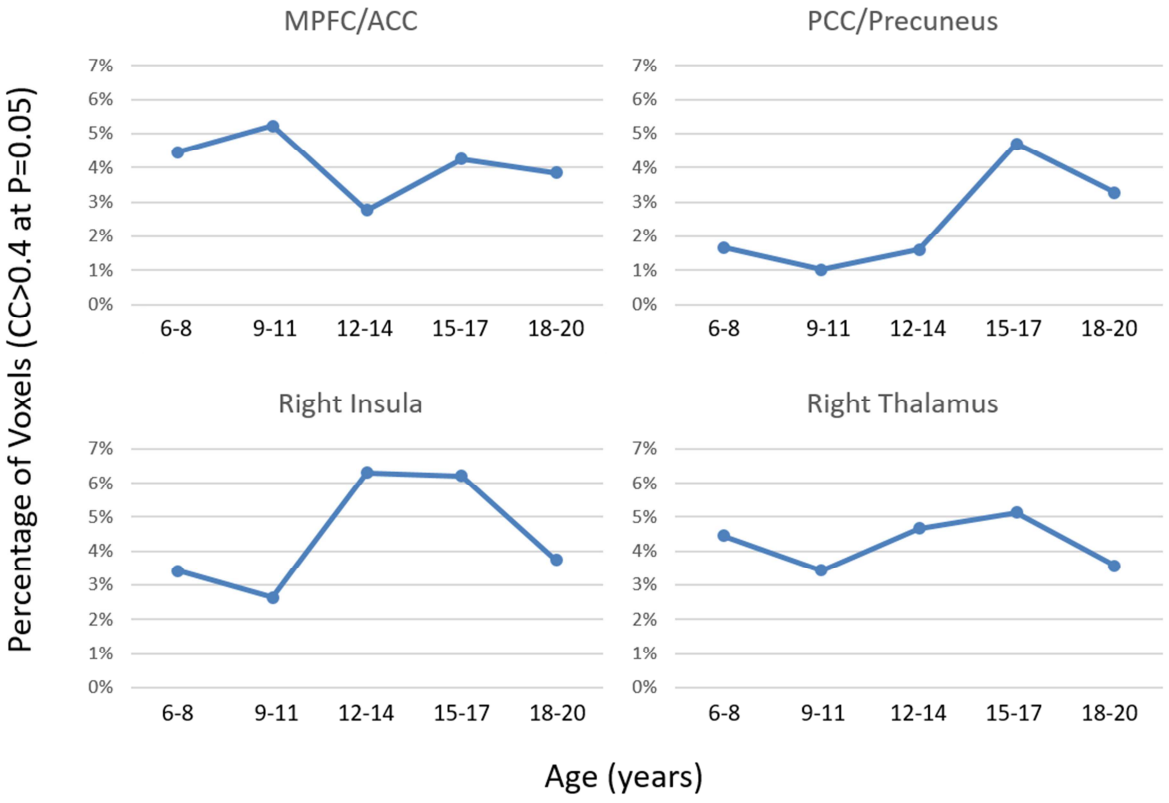

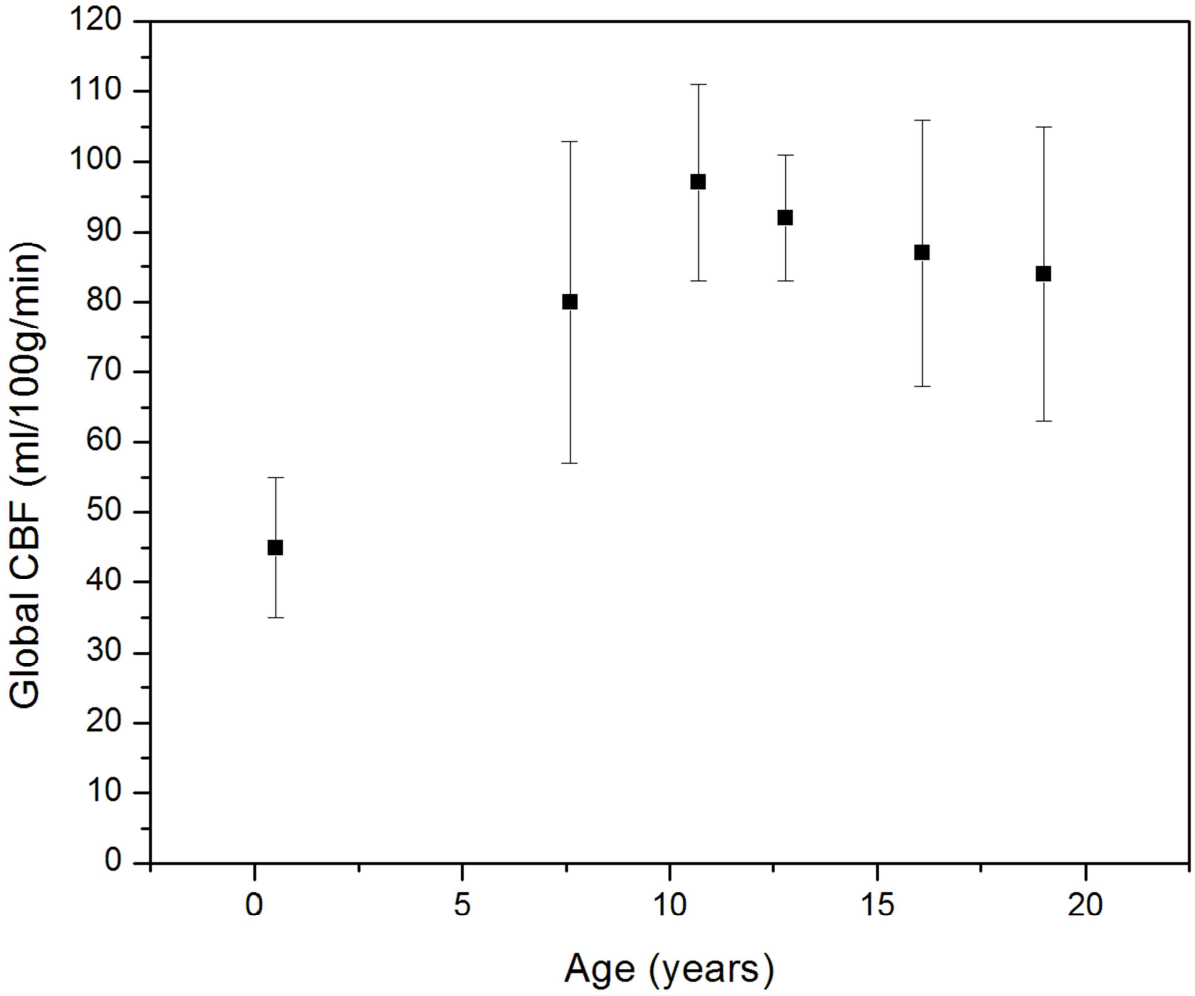
Global CBF (ml/100g/min)
120
110
100
90
80
70
60
50
40
30
20
10
0
0
5
10
15
20
Age (years)

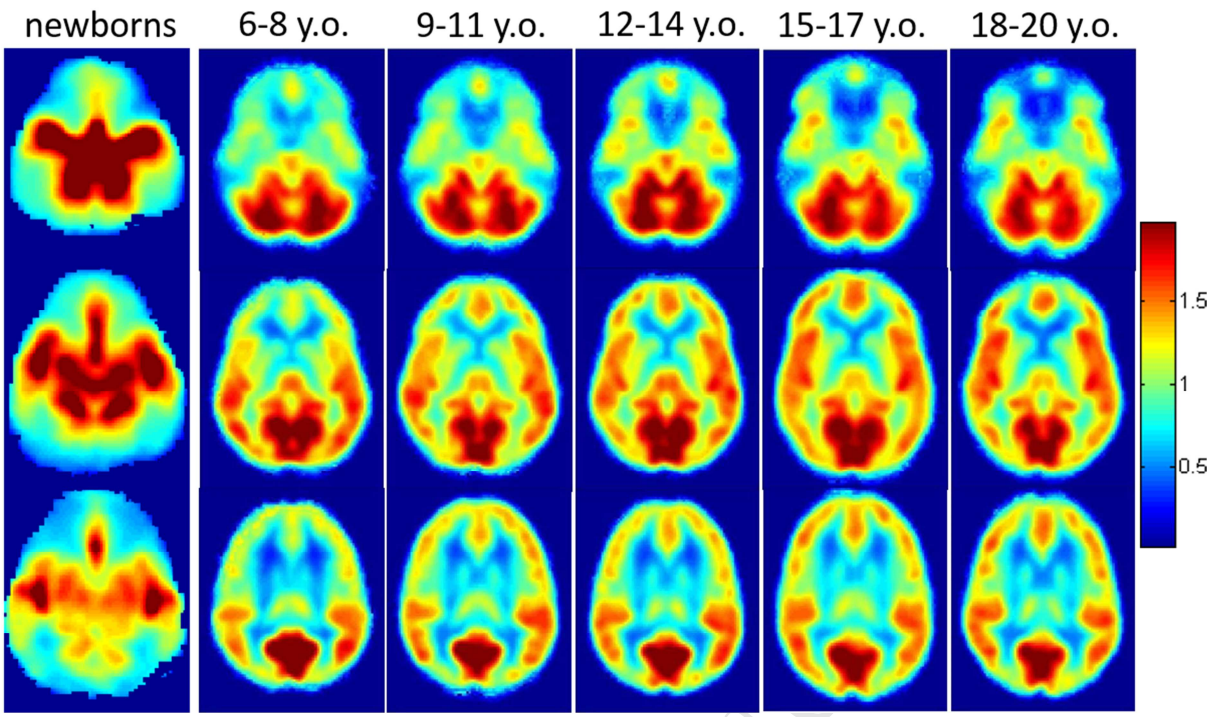

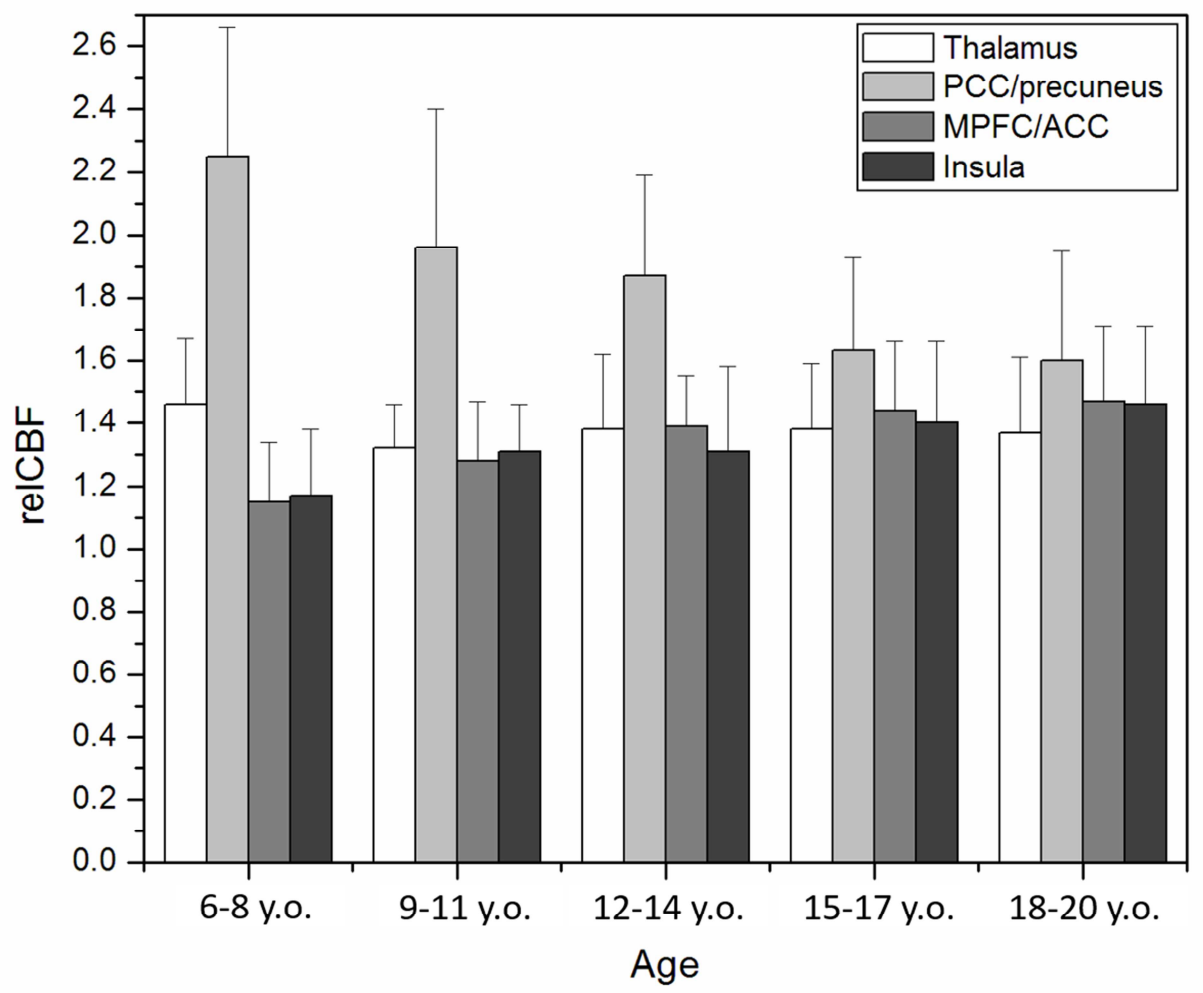
Thalamus
PCC/precuneus
MPFC/ACC
Insula
relCBF
2.6
2.4
2.2
2.0
1.8
1.6
1.4
1.2
1.0
0.8
0.6
0.4
0.2
0.0
6-8 y.o.
9-11 y.o.
12-14 y.o.
15-17 y.o.
18-20 y.o.
Age

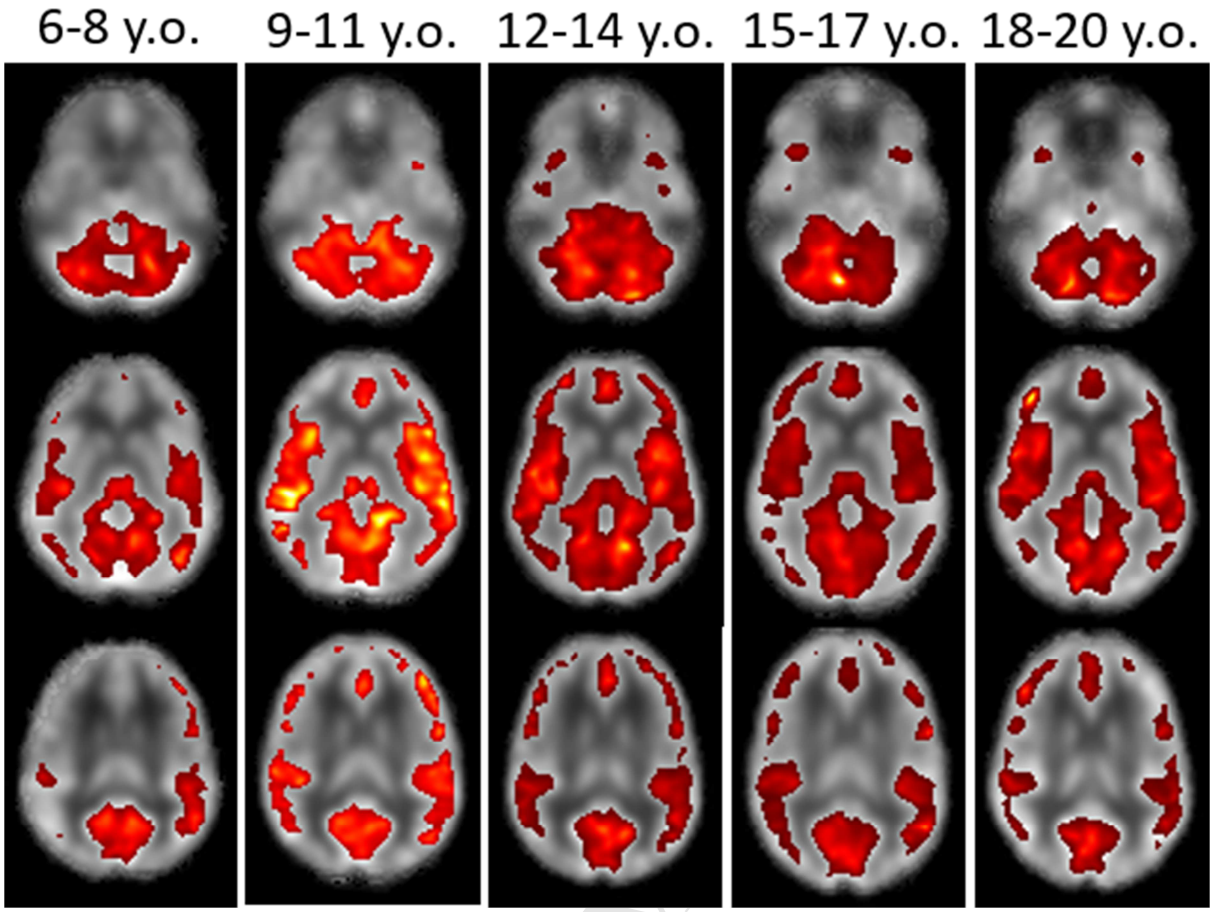

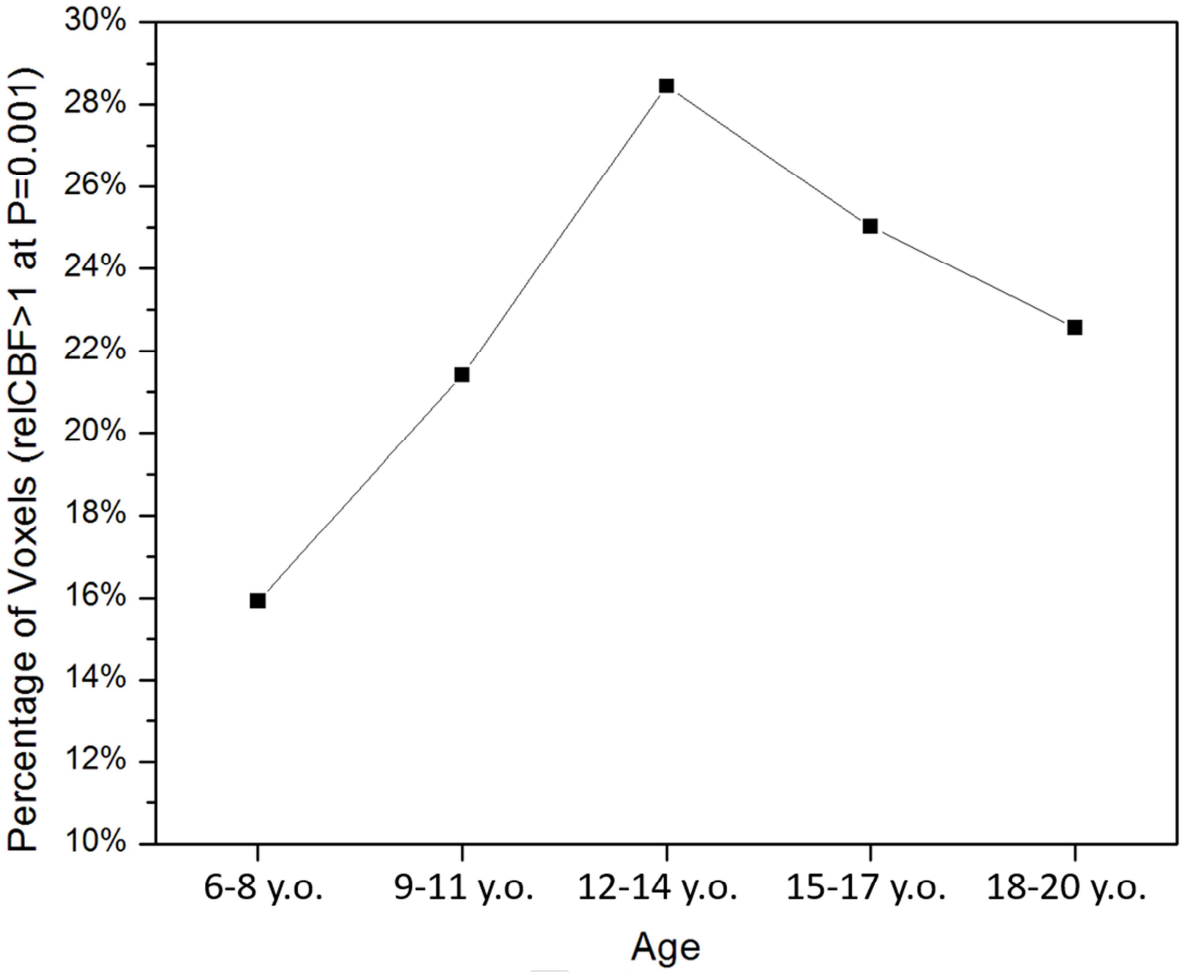
Percentage of Voxels (relCBF>1 at P=0.001)
30%
28%
26%
24%
22%
20%
18%
16%
14%
12%
10%
6-8 y.o.
9-11 y.o.
12-14 y.o.
15-17 y.o.
18-20 y.o.
Age